Skeletal Radiol (2002) 31:343–348
DOI 10.1007/s00256-002-0517-9

ARTICLE

Walter A. Wohlgemuth
Frank W. Roemer
Klaus Bohndorf

Short tau inversion recovery and three-point Dixon water–fat separation sequences in acute traumatic bone fractures at open 0.35 tesla MRI

Received: 19 October 2001
Revised: 4 December 2001
Accepted: 14 March 2002
Published online: 25 April 2002

W.A. Wohlgemuth (✉) · F.W. Roemer
K. Bohndorf
Department of Radiology,
Klinikum Augsburg, Stenglinstrasse 2,
86156 Augsburg, Germany
e-mail: w.wohlgemuth@online.de
Tel.: +49-821-42453
Fax: +49-821-4003312

Abstract *Objective:* Fat suppression can be used to improve the diagnostic confidence in traumatic bone fractures of the extremities. We compared a three-point Dixon "sandwich" water–fat separation (WFS) sequence, resulting in a water-only and a fat-only image set after one excitation, with the STIR sequence on an open 0.35 T superconductive MR system. *Design and patients:* T1-weighted, STIR (2000/40 [TR/TE]), and WFS (2000/36 [TR/TE]) MR images were prospectively obtained in 27 patients with 40 radiologically diagnosed fractures immediately after first-line treatment. Signal-to-noise (S/N) ratio, contrast-to-noise (C/N) ratio, and bone marrow edema volumes were measured together with qualitative parameters (four-point scale). *Results:* WFS was significantly superior to STIR in all quantitative parameters (better S/N ratio, $P<0.001$; better C/N ratio, $P<0.001$; larger marrow edema, $P<0.023$; Wilcoxon signed rank test). Visibility of bone marrow edema, visibility of fracture line, and preservation of anatomical details were better with the WFS sequence ($P<0.001$, $P<0.001$, $P<0.001$, respectively; ANOVA). Fat saturation was rated more homogeneous, however, with the STIR sequence (not significant; $P<0.101$). *Conclusion:* On the basis of qualitative and quantitative assessments, the three-point Dixon "sandwich" water–fat separation sequence was consistently superior to the STIR sequence in the delineation of traumatic fractures.

Keywords Magnetic resonance imaging, low field · Magnetic resonance imaging, open · Fractures, traumatic · STIR · Fat saturation · Three-point Dixon

Introduction

The growing application of magnetic resonance imaging (MRI) in traumatic extremity fractures is based on its superior detection of "occult" fractures and concomitant soft tissue injuries [1, 2, 3, 4, 5, 6, 7]. T2-weighted fat-suppression imaging with a short tau inversion recovery (STIR) sequence has an especially high proven value in the evaluation of traumatic lesions of the skeleton [8, 9, 10, 11, 12, 13] and is applicable in low-field MR systems, which have certain advantages in the setting of acute trauma. The main drawback of the STIR sequence is that all signals with a T1 identical to fat, including hematoma or contrast-enhanced tissue, are canceled out [14]. Additionally the sequence is vulnerable to motion artifacts [15] and the signal-to-noise (S/N) ratio is poor [16, 17]. In open MRI, the S/N ratio of this sequence is further decreased with the lower field strength, which can lead to an impairment of the visualization of fracture details in 0.2 T MRI [18]. As spectral fat saturation MRI is not possible in low-field MRI [19], the Dixon method [20, 21] and its modifications [22, 23, 24] are an alternative, but they have required at least two acquisitions to separate water from fat images, resulting in long scan times and problems with patient movement [25].

A modified three-point Dixon method for separation of water and fat MR images in a single scan with correction of static magnetic field inhomogeneity was implemented to overcome some of these drawbacks [26]. The purpose of our study was to evaluate the technical efficacy of the water–fat separation (WFS) sequence in acute traumatic fractures of the extremities in comparison with the STIR sequence at a field strength of 0.35 T.

Materials and methods

During a period between December 1999 and January 2000, 27 consecutive patients (15 male, 12 female; mean age 36.3 years, age range 7–76 years) with a total of 40 fractures were included in the prospective study. Inclusion criteria were admittance on an emergency basis and plain film radiographs (taken in two projections) showing an acute traumatic fracture of the appendicular skeleton. Informed consent was obtained for an additional MRI examination directly after radiographic diagnosis and first-line treatment. Patients with contraindication to MRI, known bone or joint pathology other than the recent trauma, severe soft tissue injuries or open fractures were excluded. The locations of the fractures included the distal radius (n=11), distal ulna (n=4, including one epiphyseolysis), proximal ulna (n=1), medial malleolus (n=4), lateral malleolus (n=3), distal tibia (n=5), femoral condyle (n=3), tibial plateau (n=1), tibial shaft (n=1), medial cuneiform bone (n=1), patella (n=1), talus (n=1), distal humerus (n=1), scaphoid (n=1), proximal phalanx second digit (n=1), and fourth metacarpal (n=1).

MR imaging

All MR examinations were performed on an open superconductive MR scanner (OPART, Toshiba, Japan) working at 0.35 T. The protocol consisted of a coronal STIR sequence (TR 2000 ms, TE 40 ms, TI 100 ms, thickness 3.5 mm, matrix 192×192, FoV 14×13 cm, resolution 0.7×0.7 mm, 1 signal average, acquisition time 6:30 min), a corresponding coronal WFS sequence (TR 2000 ms, TE 36 ms, thickness 3.5 mm, matrix 192×192, FoV 14×13 cm, resolution 0.7×0.7 mm, 1 signal average, acquisition time 6:30 min), resulting in a water-only and a fat-only image set, and a sagittal T1-weighted spin-echo (SE) sequence (TR 250 ms, TE 15 ms, thickness 3.0 mm, matrix 256×256, FoV 14×13 cm, resolution 0.5×0.5 mm, 2 signal averages, acquisition time 2:09 min). Imaging plane and choice of the coil were optimized for each examination according to the site and extent of the lesion and were generally consistent in the STIR and WFS sequences. The resulting images were filmed on dry laser film with optimal window width/window level settings.

Qualitative evaluation

Film reading by two independent radiologists (W.A.W., F.W.R.) included qualitative assessment of each of the following parameters (four-point scale: 1=poor, 2=fair, 3=good, 4=excellent): visibility of bone marrow edema, visibility of fracture line, preservation of anatomical details, and homogeneity of the fat saturation. The radiologists carrying out the assessment were neither masked to the sequence, due to obvious differences in the image characteristics of each sequence, nor to the plain films, due to the fact that a radiographically diagnosed fracture was the inclusion criterion.

Quantitative evaluation

Quantitative evaluation included measurement of the volume of bone marrow edema in the STIR, the water-only and the fat-only WFS image sets. The signal intensity (SI; mean value of a complete region-of-interest) of the bone marrow edema (SI_{lesion}) in the affected area, of the adjacent normal bone marrow (SI_{normal}), and of the background noise (SI_{noise}) were measured on a workstation in regions of interest with an electronic cursor encompassing a large representative area removed from any source of motion or artifact. The regions of interest ranged from 22 to 7844 mm² in size. The signal-to-noise ratio (S/N) ratio and the contrast-to-noise (C/N) ratio were calculated as follows:

$$S/N = \left[SI_{lesion}/\mathrm{StandardDeviation}(SI_{noise})\right]$$

$$C/N = \left[(SI_{lesion} - SI_{normal})/\mathrm{StandardDeviation}(SI_{noise})\right]$$

Statistical analysis used a nonparametric Wilcoxon signed-rank test of the differences in the quantitative parameters (edema volume, S/N ratio, C/N ratio) and an analysis of variance test (ANOVA) for the qualitative parameters (visibility of bone marrow edema, visibility of fracture line, preservation of anatomical details, and homogeneity of fat saturation). Significance was assessed at a P value of <0.05.

Results

Visible movement artifacts were seen in 4 cases (10%). Minor pulsation artifacts were found in 12 (30%) of the STIR sequences and in 3 (7.5%) of the WFS sequences. Due to selection of the wrong phase encoding direction, wrap-around artifacts were found in 1 patient.

Quantitative evaluation

The mean volumes of the bone marrow edema of the STIR, the WFS water-only, and the WFS fat-only sequence were 7447 mm³ (SD ±15487), 8924 mm³ (SD ±16576), and 5240 mm³ (SD ±10425), respectively. Statistical analysis showed a significantly higher edema volume in the WFS water-only sequence than in the STIR sequence (P<0.02), whereas the depicted area of bone marrow edema measured in the STIR sequence was larger than in the WFS fat-only sequence (P<0.001). Signal intensities of the measured regions-of-interest of the different sequences are provided in Table 1. The signal of bone marrow edema compared with the nearby normal hypointense bone was more hyperintense in the WFS water-only than in the STIR images, whereas the edema in the WFS fat-only sequence was more hypointense than the surrounding normal marrow. The S/N ratio and C/N ratio of the abnormal bone were both significantly higher in the WFS water-only than in the STIR images (P<0.001, and P<0.001, respectively).

Qualitative evaluation

No statistically significant interrater discrepancies were observed in the qualitative assessment. The qualitative parameters showed a similar dominance of the WFS water-only sequence in comparison with the STIR se-

Table 1 Mean value of signal intensities of bone marrow edema (SI_{lesion}), normal adjacent bone (SI_{normal}), and standard deviation of signal intensity of noise SD (SI_{noise}), as well as the signal-to-noise (S/N) and the contrast-to-noise (C/N) ratio of 40 fractures for short tau inversion recovery (STIR), water–fat separation (WFS) water-only, and WFS fat-only image sets (mean; ±SD)

	SI_{lesion}	SI_{normal}	SD (SI_{noise})	S/N ratio	C/N ratio
STIR	10215 (±6893)	2027 (±1573)	144	19.40 (±13.72)	15.57 (±12.18)
WFS water-only	44201 (±21819)	11783 (±6348)	341	36.46 (±20.05)	26.61 (±16.12)
WFS fat-only	16641 (±11797)	49714 (±14199)	323	17.35 (±15.53)	–30.04 (±13.78)

Table 2 Results of the qualitative (four-point scale:1=poor, 2=fair, 3=good, 4=excellent) statistical comparison (ANOVA) of the short tau inversion recovery (STIR) and the water–fat separation (WFS) water-only image sets (mean; variance) in 40 fractures

	Visibility of bone marrow edema	Visibility of fracture line	Preservation of anatomical details
STIR	3.125 (0.948)	2.014 (1.164)	2.292 (0.317)
WFS water-only	3.75 (0.179)	3.0 (0.686)	3.347 (0.297)
Statistical difference	$P<0.001$	$P<0.001$	$P<0.001$

quence. The ANOVA analysis revealed a statistically significant superiority of the WFS water-only sequence over the STIR sequence in terms of visibility of the bone marrow edema, the visibility of fracture line, and the preservation of anatomical details (Table 2). Fat saturation homogeneity was not significantly different ($P<0.101$) between STIR (mean 3.66; variance 0.229) and WFS (mean 3.45; variance 0.334). There were two false positive findings in the radiographs (posterior portion of the distal tibia, $n=1$; lateral femoral condyle, $n=1$) and two missed fractures in the MR images (both avulsion fractures of the styloid process of ulna).

Discussion

The "sandwich" type three-point Dixon method [26] achieves water–fat separation (WFS) in a single scan by acquiring three "sandwiched" echoes after a single radiofrequency (RF) excitation (Fig. 1). The chemical-shift-based method takes advantage of the fact that, due to the lower precession frequency at low field strength, the time for water and fat protons to make the transition from in-phase to out-of-phase is longer (about 9.6 ms at 0.35 T compared with 2.25 ms at 1.5 T), allowing the possibility of acquiring both in-phase and out-of-phase data after a single excitation [27]. This eliminates the typical image subtraction movement artifacts of the conventional three-point Dixon method [25] and has special advantages when applied in musculoskeletal radiology [27]. As our study showed, the S/N ratio increases significantly compared with the STIR sequence, as the images are calculated out of three echoes after one RF excitation. Two different image sets are reconstructed out of a single scan: a water-only and a fat-only image set. The character of the WFS fat-only images is similar to a

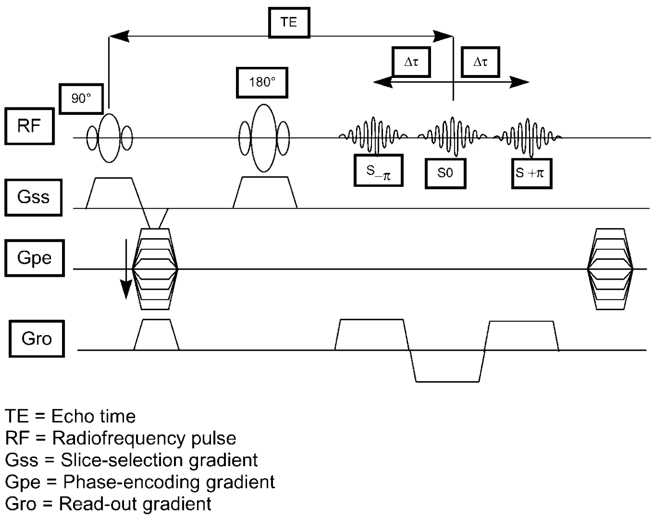

Fig. 1 Timing diagram of the water–fat separation (WFS) sequence. A single radiofrequency echo is "sandwiched" between two gradient echoes (±10 ms). The gradient echoes are used to determine the B(0) distribution and to produce out-of-phase images. *TE* echo time, *RF* radiofrequency pulse, *Gss* slice-selection gradient, *Gpe* phase-encoding gradient, *Gro* read-out gradient

T1-weighted image (edema is hypointense to the surrounding hyperintense bone marrow, the fracture line is very hypointense). This potentially would make acquisition of an additional T1-weighted sequence for visualization of the fracture line unnecessary (Fig. 2). Saving acquisition time is especially worthwhile in an emergency setting, and thus we envisage a practical potential of the sequence in this field. However, a systematic comparison of a T1-weighted SE sequence with the WFS fat-only image set was not performed in our study. This would have required acquisition of an additional T1-weighted

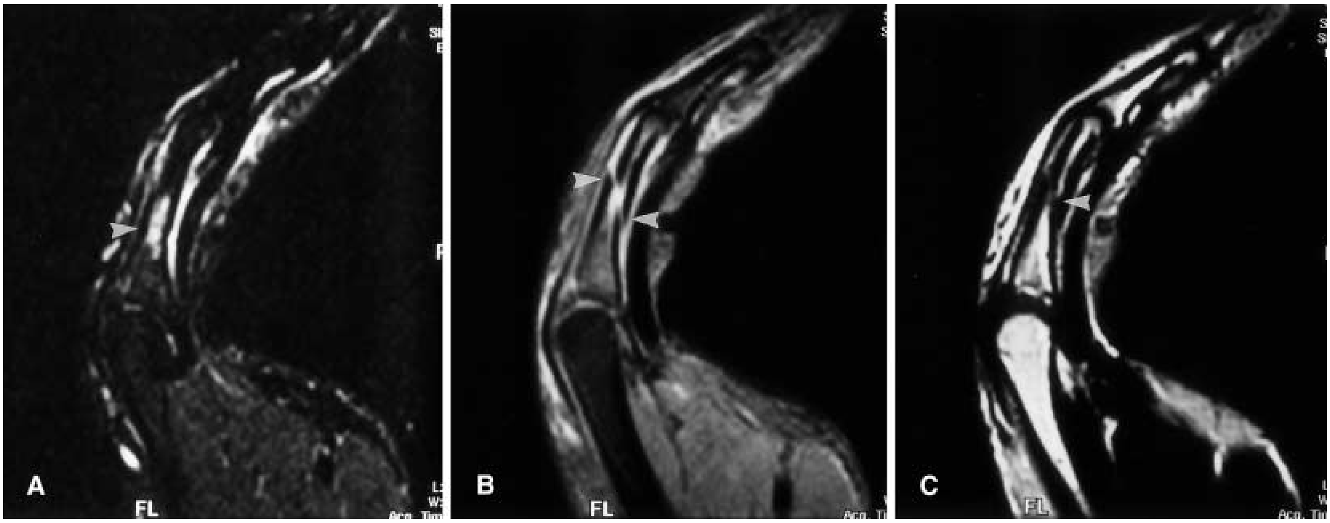

Fig. 2A–C. Patient with a diaphyseal fracture of the proximal phalanx of the fourth digit. **A** Sagittal STIR image shows bone marrow edema (*arrowhead*) but no clear fracture line is visible. **B** Sagittal WFS water-only image visualizes cortical disruption (*arrowheads*). **C** WFS fat-only image shows the fracture as a black line (*arrowhead*)

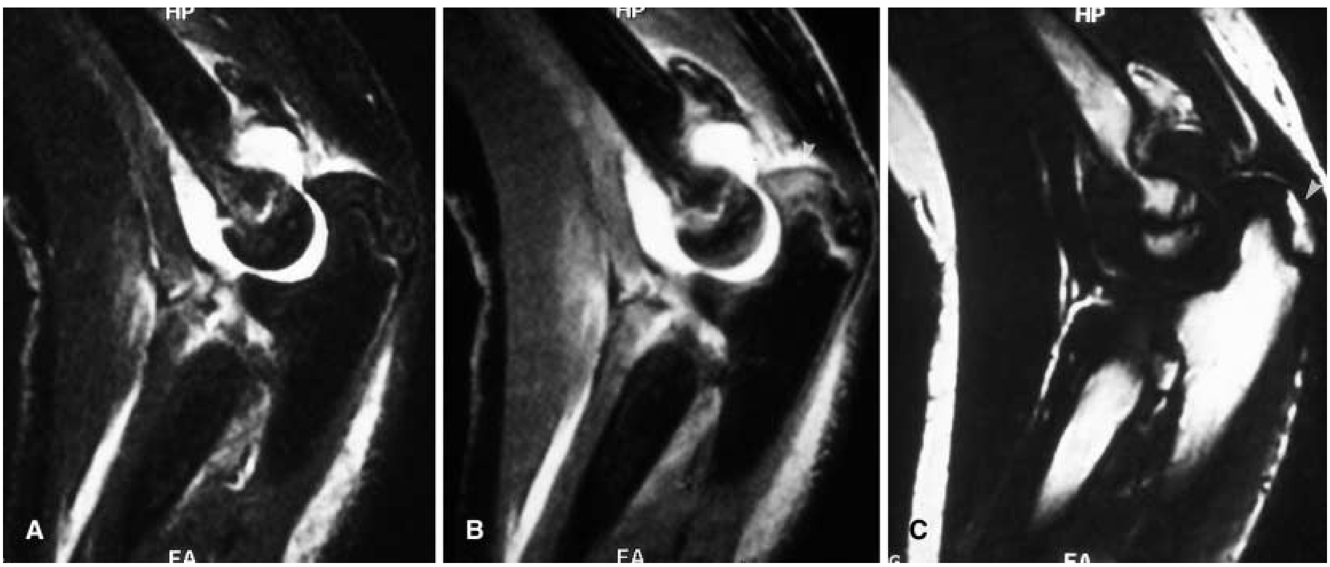

Fig. 3A–C A 12-year-old boy with a fracture of the coronoid process of the ulna. **A** Sagittal STIR image reveals a joint effusion. **B** Sagittal WFS water-only image shows additional edema of the olecranon (*arrow*). **C** In the corresponding WFS fat-only image partial ossification of the olecranon with fatty bone marrow (*arrow*) is visible as well

SE sequence in the same plane as the WFS sequence, resulting in an unacceptable increase in acquisition time in our patients with acute traumatic fractures. The character of the WFS water-only images is similar to the STIR sequence (marrow edema is hyperintense to the normal hypointense bone). The results of our study show an obvious superiority of the WFS water-only sequence in comparison with the STIR sequence in the qualitative and quantitative parameters. Additionally, the WFS sequence showed fewer artifacts than the STIR sequence. It is applicable in distal extremities with irregular anatomy and high susceptibility differences (Fig. 3), where frequency-selective fat saturation regularly fails [25, 28]. The higher S/N ratio of the WFS images compared with the STIR images allows for a better depiction of soft tissue pathology (Fig. 4). Acute fractures may show no or only minimal bone marrow edema, thus making the diagnosis with STIR images more difficult than with the WFS images given the additional T1-like contrast information of a fat-only image set. In the absence of any bone marrow edema, a fracture line can clearly be depicted in the WFS

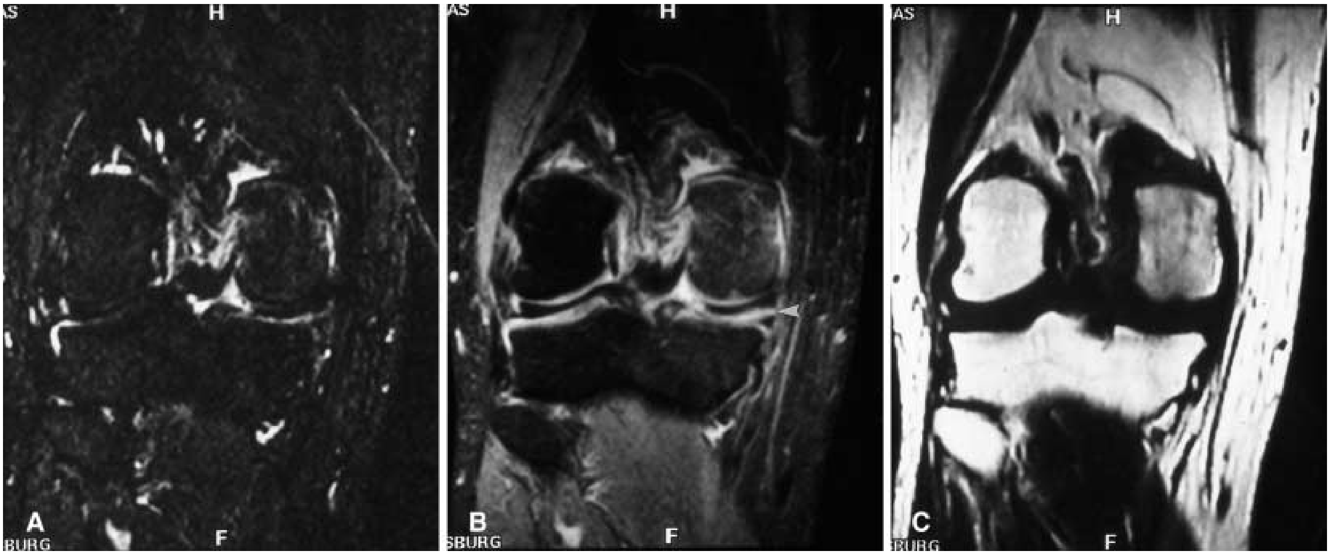

Fig. 4A–C Patient with a femoral condyle fracture. **A** Coronal STIR image fails to show the full extent of bone marrow edema. **B** Corresponding WFS water-only image (0.35 T) shows both condylar and tibial bone marrow edema. Due to the good signal-to-noise ratio, an additional meniscal tear is seen (*arrow*). **C** WFS fat-only image demonstrates marrow edema as subtle signal loss in the medial femoral condyle

fat-only images as a black line in the very hyperintense bone marrow. Fracture lines are visualized in STIR images as subtle hypointense lines in the very hyperintense bone marrow edema and can be seen in only 50% of traumatic fractures [9].

Limitations of our study are the heterogeneous patient group with small numbers of examinations in various regions, and the fact that only the technical, not the diagnostic efficacy [29] was assessed.

In summary, the WFS sequence applied in low-field open MRI not only consistently demonstrated traumatic fractures seen radiographically, but was clearly superior to the STIR sequence in terms of visibility of the bone marrow edema, the visibility of fracture line, and the preservation of anatomical details. Nevertheless it showed a tendency to less homogeneous fat saturation than the STIR sequence.

References

1. Feldman F, Staron R, Zwass A, Rubin S, Haramati N. MR imaging: its role in detecting occult fractures. Skeletal Radiol 1994; 23:439–444.
2. Yao L, Joong KL. Occult intraosseous fracture: detection with MR imaging. Radiology 1988; 167:749–751.
3. Brossman J, Biederer J, Heller M. MR imaging of musculoskeletal trauma to the pelvis and the lower limb. Eur Radiol 1999; 9:183–191.
4. Rogers LF. Occult is a matter of definition. AJR Am J Roentgenol 1999; 172:283.
5. Deutsch AL, Mink JH, Shellock FG. Magnetic resonance imaging of injuries to bone and articular cartilage: emphasis on radiographically occult abnormalities. Orthop Rev 1990; 19:66–75.
6. Ohashi K, Brandser EA, el-Khoury GY. Role of MR imaging in acute injuries to the appendicular skeleton. Radiol Clin North Am 1997; 35:591–613.
7. Eustace S, Keogh C, Blake M, Ward RJ, Oder PD, Dimasi M. MR imaging of bone oedema: mechanisms and interpretation. Clin Radiol 2001; 56:4–12.
8. Breitenseher MJ, Metz VM, Gilula LA, Gaebler C, Kukla C, Fleischmann D, Imhof H, Trattnig S. Radiographically occult scaphoid fractures: value of MR imaging in detection. Radiology 1997; 203:245–250.
9. Meyers SP, Wiener SN. Magnetic resonance imaging features of fractures using the short tau inversion recovery (STIR) sequence: correlation with radiographic findings. Skeletal Radiol 1991; 20:499–507.
10. Van Gelderen WF, al-Hindawi M, Gale RS, Steward AH, Archibald CG. Significance of short tau inversion recovery sequence in the management of skeletal injuries. Australas Radiol 1997; 41:13–15.
11. Mirowitz SA, Apicella P, Reinus WR, Hammerman AM. MR imaging of bone marrow lesions: relative conspicuousness on T1-weighted, fat-suppressed T2-weighted, and STIR images. AJR Am J Roentgenol 1994; 162:215–221.
12. Pui MH, Goh PS, Choo HF, Fok EC. Magnetic resonance imaging of musculoskeletal lesions: comparison of three fat-saturation pulse sequences. Australas Radiol 1997; 41:99–102.
13. Pozzi Mucelli R, Cova M, Shariat-Razavi I, Zucconi F, Ukmar M, Longo R. Confronto in Risonanza Magnetica tra sequenze Spin-echo e sequenze con soppressione del grasso nelle malattie dello scheletro. Radiol Med 1997; 93:504–509.
14. Vanel D, Dromain C, Tardivon A. MRI of bone marrow disorders. Eur Radiol 2000; 10:224–229.

15. Pui MH, Chang SK. Comparison of inversion recovery fast spin-echo (FSE) with T2-weighted fat-saturated FSE and T1-weighted MR imaging in bone marrow lesion detection. Skeletal Radiol 1996; 25:149–152.
16. Shuman WP, Baron RL, Peters MJ, Tatioli PK. Comparison of STIR and spin-echo MR imaging at 1.5 T in 90 lesions of the chest, liver, and pelvis. AJR Am J Roentgenol 1989; 153:1104–1105.
17. Simon JH, Szumowski J. Proton (fat/water) chemical shift imaging in medical magnetic resonance imaging: current status. Invest Radiol 1992; 27:865–874.
18. Breitenseher MJ, Trattnig S, Gabler C, Happel B, Bankier A, Kukla C, Rand T, Imhof H. MRT bei radiologisch okkulten Kahnbeinfrakturen. Erste Erfahrungen von 1.0 Tesla (Ganzkörper-Mittelfeldgerät) versus 0.2 Tesla (dediziertes Niederfeldgerät). Radiologe 1997; 37:812–818.
19. Delfault EM, Beltran J, Johnson G, Rousseau J, Marchandise X, Cotten A. Fat suppression in MR imaging: techniques and pitfalls. Radiographics 1999; 19:373–382.
20. Dixon WT. Simple proton spectroscopic imaging. Radiology 1984; 153:189–194.
21. Lee JKT, Dixon WT, Ling D, Levitt RG, Murphy WA. Fatty infiltration of the liver demonstration by proton spectroscopic imaging. Radiology 1984; 153:195–201.
22. Yeung HN, Kormos DW. Separation of true fat and water images by correcting magnetic field inhomogeneity in situ. Radiology 1986; 159:783–786.
23. Williams SCR, Horsfield MA, Hall LD. True water and fat MR imaging with the use of multiple-echo acquisition. Radiology 1989; 173:249–253.
24. Szumowski J, Coshow W, Li F, Coombs B, Quinn SF. Double-echo-three point Dixon method for fat suppression MRI. Magn Reson Med 1995; 34:120–124.
25. Maas M, Dijkstra PF, Akkerman EM. Uniform fat suppression in hands and feet through the use of two-point Dixon chemical shift MR imaging. Radiology 1999; 210:189–193.
26. Zhang W, Goldhaber DM, Kramer D. Separation of water and fat MR images in a single scan at 0.35 T using “sandwich” echoes. J Magn Reson Imaging 1996; 6:909–917.
27. Bredella MA, Losasso C, Moelleken SC, Hügli RW, Genant HK, Tirman PFJ. Three-point Dixon chemical-shift imaging for evaluating articular cartilage defects in the knee joint on a low-field-strength open magnet. AJR Am J Roentgenol 2001; 177:1371–1375.
28. Anzai Y, Lufkin RB, Jabour BA, Hanafee WN. Fat-suppression failure artifacts simulating pathology on frequency-selective fat-suppression MR images of the head and neck. AJNR Am J Neuroradiol 1992; 13:879–884.
29. Thornbury JR. Clinical efficacy of diagnostic imaging: love it or leave it. AJR Am J Roentgenol 1994; 162:1–8.